

## Development and Characterization of PCL/Nano-Hydroxyapatite/PEG Electrospun Membranes for Improved Guided Bone Tissue Regeneration in Dental Applications

Aditya Dotiya<sup>1</sup>, Sahana selvaganesh<sup>2</sup>, Abhishek Dotiya<sup>3</sup>, Thiyaneswaran Nesappan<sup>4</sup>

<sup>1,3</sup>Resident, Department of Implantology, Saveetha Dental College and Hospitals, Saveetha Institute of Medical and Technical Science, Saveetha University, Chennai, India

<sup>2</sup>Assistant professor, Department of Implantology, Saveetha Dental College and Hospitals, Saveetha Institute of Medical and Technical Science, Saveetha University, Chennai, India

<sup>4</sup>Professor, Saveetha Dental College and Hospitals, Saveetha Institute of Medical and Technical Science, Saveetha University, Chennai, India

**\*Corresponding Author:**

Dr. Sahana Selvaganesh

**Cite this paper as:** Aditya Dotiya, Sahana selvaganesh, Abhishek Dotiya, Thiyaneswaran Nesappan, (2025) Assessment Of Management Strategies In Alcoholic Liver Disease Patients With Hypertension Or Diabetes Mellitus. *Journal of Neonatal Surgery*, 14 (17s), 413-421.

### ABSTRACT

**Background:** Dental implantology relies on the presence of healthy bone tissue at the implant site. Guided bone tissue regeneration (GBTR) techniques enhance bone volume and quality, crucial for implant stability. Electrospun membranes, with their high surface area and porosity, are promising for GBTR due to their ability to mimic the extracellular matrix. **Aim:** This study investigates the preparation and characterization of electrospun membranes composed of poly( $\epsilon$ -caprolactone) (PCL), nano-hydroxyapatite (nano-HAp), and polyethylene glycol (PEG) for guided bone tissue regeneration in dentistry.

**Methodology:** PCL pellets were dissolved in chloroform with PEG to enhance electrospinnability. Nano-HAp particles were dispersed in the PCL solution. Electrospinning was employed to fabricate nanofibrous membranes. Characterization included SEM, FTIR, mechanical testing, wettability tests, and cell viability analysis using MG-63 cells through confocal microscopy.

**Results:** SEM confirmed the formation of nanofibrous structures with porous surfaces. FTIR validated the incorporation of nano-HAp. The experiment group showed higher mean tensile strength (4.70 MPa) and strain (12.68%) than the control (3.64 MPa and 10.22%). The experiment group exhibited a lower water contact angle (63.40°) compared to the control (90.00°). Confocal microscopy indicated superior cell attachment and proliferation on the experiment scaffolds. **Discussion:** The study demonstrated that electrospun membranes with PEG and nano-HAp significantly enhance mechanical properties, wettability, and biocompatibility compared to PCL-only membranes. The improved tensile strength, strain, and lower contact angle suggest better material integrity and hydrophilicity, essential for promoting cell adhesion and bone regeneration. Superior cell attachment and proliferation observed in the experiment group indicate that these membranes are more effective in supporting bone tissue regeneration.

**Conclusion:** PCL + PEG + nano-HAp membranes demonstrate enhanced mechanical properties, wettability, and biocompatibility, making them suitable for guided bone tissue regeneration in dentistry.

**Keywords:** Electrospinning, poly( $\epsilon$ -caprolactone), nano-hydroxyapatite, polyethylene glycol, guided bone tissue regeneration, dental implants, biocompatibility, mechanical properties, wettability, cell viability.

### 1. INTRODUCTION

Dental implantology has revolutionized modern dentistry by providing an effective solution for the replacement of missing teeth. However, successful implantation relies heavily on the presence of a healthy and adequate volume of bone tissue at the implant site (Cicciù et al., 2023). In cases where the bone quantity or quality is compromised due to trauma, periodontal disease, or congenital anomalies, guided bone tissue regeneration (GBTR) techniques play a vital role in facilitating bone regeneration and supporting implant stability (Kandhari et al., 2023; Tolstunov, 2022).

Electrospun membranes have shown great potential in dental applications for GBTR due to their unique characteristics, including high surface area, porosity, and tunable physical and biological properties (Berton et al., 2019). In this study, we

focus on the preparation and characterization of electrospun membranes composed of poly( $\epsilon$ -caprolactone) (PCL), nano-hydroxyapatite (nano-HAp), and polyethylene glycol (PEG) for guided bone tissue regeneration in dentistry (Mahmoud et al., 2023; Watcharajittanont et al., 2023) (Shankar et al., 2024).

Poly( $\epsilon$ -caprolactone) (PCL), a biodegradable polymer with excellent biocompatibility, has been extensively investigated in the field of dental tissue engineering (Calciolari et al., 2023). Its slow degradation rate aligns with the bone healing process, providing a supportive matrix for cellular attachment, proliferation, and new bone formation (Priya Veeraraghavan, Rilah, et al., 2023). By incorporating nano-hydroxyapatite (nano-HAp) into the PCL matrix, the electrospun membranes can offer enhanced osteoconductivity and mimic the mineral composition of natural bone, promoting rapid and effective bone regeneration at the implant site (Duraisamy & Senior Lecturer, Department of Prosthodontics and Implantology, Saveetha Dental College and Hospitals, Saveetha Institute of Medical and Technical Sciences, 2021; Wu et al., 2023) (Lee et al., 2023).

Polyethylene glycol (PEG), a hydrophilic polymer, is commonly used as an additive in electrospinning to improve the processability and biocompatibility of the resulting membranes (Givens, 2008). The addition of PEG enhances the electrospinnability of the PCL solution, enabling the formation of fine, uniform fibers with improved mechanical properties. Moreover, PEG imparts hydrophilicity to the membranes, facilitating cell adhesion, nutrient diffusion, and waste removal at the site of bone regeneration (Das & Gebru, 2018).

The electrospinning technique allows for the fabrication of nanofibrous membranes with a structure resembling the extracellular matrix (ECM), promoting cellular attachment, migration, and proliferation (Watcharajittanont et al., 2023) (Liang et al., 2024). The fiber diameter, alignment, and morphology of the electrospun membranes can be precisely controlled by adjusting the electrospinning parameters (Ramsundar et al., 2023; Rieshy et al., 2023; Singh et al., 2023). The resulting membranes provide a scaffold that supports cellular ingrowth and differentiation, facilitating the formation of new bone tissue (Pavithra et al., 2023; Shenoy et al., 2023; Thomas & Jain, 2023).

Characterization of the electrospun membranes is essential to evaluate their suitability for guided bone tissue regeneration in dentistry (Tripathi et al., 2023) (Liang et al., 2024; Su, 2020). Scanning electron microscopy (SEM) enables the examination of membrane morphology, fiber distribution, and interconnectivity, providing insights into their structural characteristics (Doshi et al., 2023; Lampl et al., 2023; Pandiyan et al., 2023). Fourier transform infrared spectroscopy (FTIR) helps identify the chemical composition and interactions between the polymer components, confirming the presence of nano-HAp within the membranes. Mechanical testing assesses the tensile strength and flexibility of the membranes, ensuring their ability to withstand masticatory forces and maintain stability during the healing process.

## **2. MATERIALS AND METHODOLOGY:**

### **2.1. Materials and Methods:**

The study was conducted in Green Lab, Saveetha Dental College, in Chennai in the year 2023.

Poly( $\epsilon$ -caprolactone) (PCL) pellets with a molecular weight of  $M_n$  80,000 and Polyethylene glycol (PEG) with a molecular weight of  $M_n$  6000 were procured from Sigma-Aldrich (Chennai Branch).

Nano-hydroxyapatite (nano-HAp) particles with an average particle size of 10-100 nm were produced biomimetically using simulated body fluid. Chloroform was used as an organic solvent.

### **2.2. Preparation of PCL Solution:**

0.2 g PCL pellets were taken, They were then dissolved in 2ml organic solvent (chloroform) to a concentration of 10% w/v. The solution was stirred using a magnetic stirrer until complete dissolution was achieved. 40 mg of PEG was added to the PCL solution to enhance electrospinnability and biocompatibility. Stir the solution to ensure homogeneity.

### **2.3. Preparation of Nano-HAp-Loaded PCL Solution:**

60 mg of nano-HAp particles were weighed according to the desired loading concentration. The weighed nano-HAp particles were added to the prepared PCL solution. The solution was stirred using a magnetic stirrer for a sufficient period to achieve a homogeneous dispersion of nano-HAp within the PCL solution.

### **2.4. Electrospinning Process:**

The electrospinning apparatus was set up in a controlled environment to minimize electrostatic interference. The metal collector plate was attached to the high-voltage power supply and grounded. The PCL or nano-HAp-loaded PCL solution were loaded into a syringe fitted with a blunt-tipped needle. The distance between the needle tip and the collector plate was adjusted, typically in the range of 20 to 30 cm, depending on the desired fiber morphology and diameter. A high voltage (e.g., 5-50 kV) was then applied to the needle using the high-voltage power supply. Gradually and uniformly extrude the nano-HAp-loaded PCL solution from the syringe using a syringe pump at a predetermined flow rate which can be controlled using the gauge of the needle and the voltage.

The electrospinning procedure was continued till the desired membrane thickness was achieved. After electrospinning, the electrospun membrane was carefully removed from the collector plate using scissors or a cutting tool.

The electrospun membrane was placed in a vacuum oven at a temperature of 60°C to remove any residual solvent and promote further drying and solidification. Once fully dried, the electrospun membrane was stored in an airtight container until further use.

### **2.5. Morphology analysis**

Scanning electron microscopy (SEM, JSM-7401F) was used to analyze the morphologies of the electrospun PCL/GE and HAp-PCL/GE fibers.

### **2.6. Mechanical testing**

A universal testing machine (UTM) was used to measure the electrospun fibrous membranes' tensile strength (Jawaid et al., 2018). Every sample was created using electrospun fibrous membranes in the shape of a rectangle with dimensions of 5 by 20 mm for both width and length. A digital micrometer was used to measure the sample thicknesses. For any given type of electrospun fibrous membrane, at least five samples were stretched until they broke. 500 gf load cells were used to take the measurements. At a deformation speed of 0.5 mm/s, load-deformation data were obtained, and the load-deformation curve was used to build the stress-strain curve of the nanofibrous structure.

### **2.7. Water contact angle (Wettability Testing)**

A device called the EasyDrop Contact Angle Measuring System was used to assess and compare the hydrophilicities of electrospun PCL/GE and HAp-PCL/GE membranes. To measure the water contact angle (Hilal et al., 2017), the membranes were set up on a sample stage, and water was automatically dripped onto the sample's mesh surface. Making sessile droplets required the use of a fine needle. As the sample table is rotated upward and downward again, a drop is created at the needle's tip and then collected up by the mesh surface. One side of the drop is lit, and the image is captured by a camera on the other. After being saved to a computer, the drop image was displayed on a monitor. To determine the contact angle, the DSA software examines the drop image.

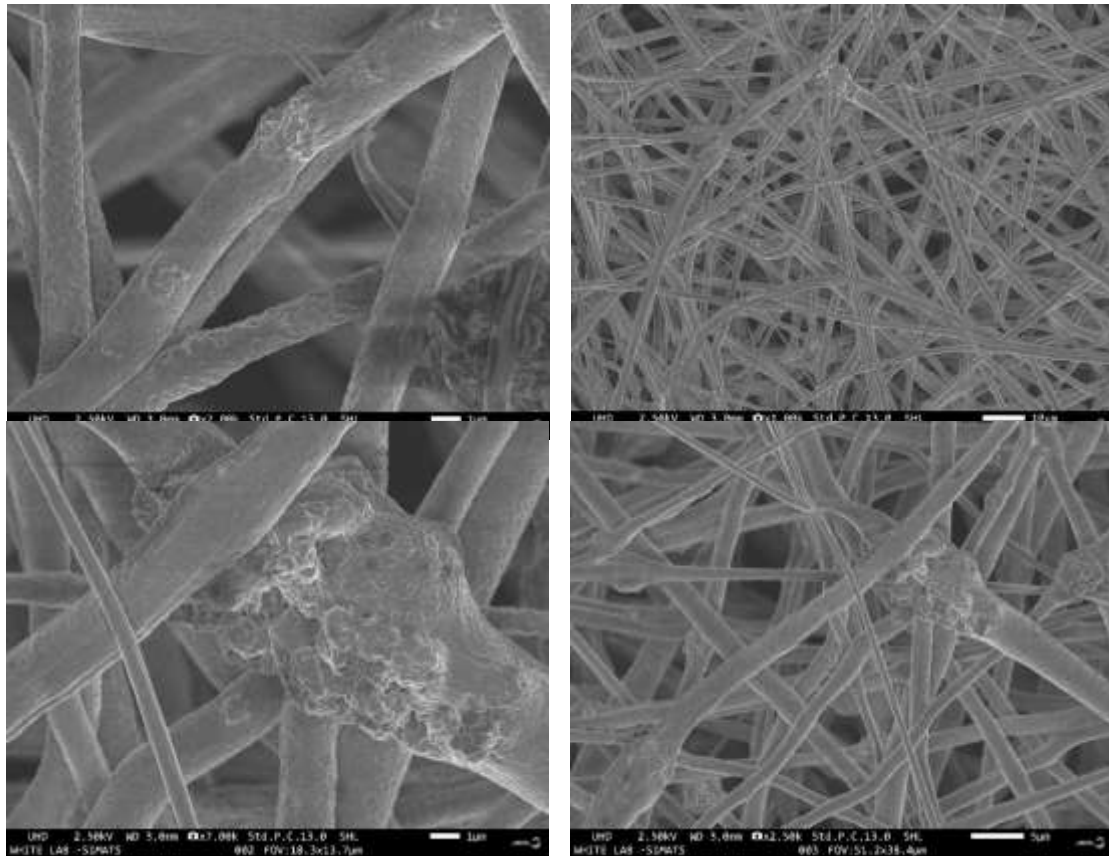
### **2.8. Cell Viability and Confocal analysis**

Electrospun nanofibers were initially sterilized under UV light for 6 h per side, sterilized further with 70% ethanol (30 min), washed with phosphate-buffered saline (PBS), and finally soaked in DMEM (Dulbecco's Modified Eagle Medium) for 1 h. MG-63 cells were seeded on 1 mm of the scaffold (20 mm in diameter) at a density of 104 cells/cm<sup>2</sup> in a 24-well plate culture medium with 10% fetal bovine serum and 1% penicillin-streptomycin. Confocal microscopy was performed to observe the growth of the MG-63 cell seeded onto the PCL/GE and HAp-PCL/GE scaffolds, respectively. Briefly, after 1 day, 3 days, and 7 days of culture, the PCL/GE and 50% HAp-PCL/GE scaffolds were rinsed with PBS twice and fixed in 4% paraformaldehyde (Sigma-Aldrich) for 15 min at room temperature, permeability in PBS containing 0.25% Triton X-100 (Sigma-Aldrich) for 10 min and blocked in 2.5% BSA for 30 min. The cells were immunostained by using (FITC-conjugated phalloidin (25 µg/ml) for 2 h at room and anti-collagen type I antibody (1:100 dilutions) overnight at 4 °C. Nuclei were counterstained with DAPI. Finally the scaffolds were mounted onto glass slides and visualized under a confocal fluorescent microscope (FV10i-W) using 10 (low magnification) and 60 (high magnification) objectives.

## **3. RESULTS**

### **3.1. Morphologies of electrospun PCL and HAp-loaded membranes:**

Scanning electron microscopy (SEM) images of electrospun polycaprolactone (PCL) incorporated with nano hydroxyapatite (nano HAp) particles reveal structural details and morphological characteristics at the micro- and nano-scale. These images exhibited an intricate network of PCL fibers interspersed with uniformly dispersed nano HAp particles, highlighting their distribution and interaction within the matrix. The SEM micrographs provide valuable insight into the fiber diameter, orientation, and alignment, as well as the dispersion and agglomeration of nano HAp particles. The Unwoven matrix of fibers with triangular voids represent the extracellular matrix and allow maximum surface area for the osteoblast to adhere.



3.2. Mechanical testing

Mechanical Property	Control Group (Mean ± SD)	Experimental Group (Mean ± SD)	p-value
Tensile Strength (MPa)	3.64 ± 0.10	4.70 ± 0.14	0.001*
Tensile Strain (%)	10.22 ± 0.17	12.68 ± 0.42	0.004*

\*Significance: P-value is less than 0.05.

The higher tensile strength and strain observed in the experiment group are indicative of better material integrity, which is essential for maintaining scaffold stability under physiological conditions. The statistically significant p-values obtained from the t-tests confirm that these improvements are not due to random variation but are a direct result of the material modifications.

3.3. Wettability Test:

The water contact angle was measured for 5 samples from each group.

Property	Control Group (Mean $\pm$ SD)	Experimental Group (Mean $\pm$ SD)	p-value
Water Contact Angle ( $^{\circ}$ )	90.00 $\pm$ 1.58	63.40 $\pm$ 1.14	0.0145*

\*Significance: P-value is less than 0.05.

The wettability tests showed a marked decrease in the water contact angle for the experimental group compared to the control group. The control group had a mean water contact angle of  $90.00^{\circ}$  (SD = 1.58), while the experiment group had a mean water contact angle of  $63.40^{\circ}$  (SD = 1.14). The lower contact angle signifies enhanced hydrophilicity, which is crucial for promoting cell adhesion, proliferation, and differentiation. Improved wettability facilitates better nutrient diffusion and waste removal, thereby creating a more favorable environment for cellular activities necessary for bone regeneration.

### 3.4. Cell Viability and Confocal analysis

Electrospun nanofibers were tested for cell viability using MG-63 cells seeded on both control (PCL only) and experiment (PCL + PEG + Nano HAp) scaffolds. The scaffolds underwent sterilization with UV light, ethanol, and PBS washes before soaking in DMEM. MG-63 cells were then cultured on the scaffolds, and confocal microscopy was used to observe cell growth on days 1, 3, and 7.

In the control group, moderate cell attachment was observed on day 1, with cells starting to spread. By day 3, cell proliferation increased, forming a more interconnected network. By day 7, significant cell growth resulted in dense cell layers covering most of the scaffold surface. In contrast, the experiment group showed high cell attachment and rapid cell spreading on day 1. By day 3, there was markedly increased cell proliferation and faster network formation compared to the control group. By day 7, the experiment group exhibited extensive cell growth with well-formed, dense, multi-layered structures covering the scaffold surface completely.

Confocal microscopy images confirmed these observations, showing sparse cell distribution in the control group on day 1 and high cell density in the experiment group. By day 7, the control group had dense cell layers, while the experiment group had multi-layered dense structures. These results suggest that the PCL + PEG + Nano HAp scaffolds significantly enhance cell attachment and proliferation, making them more suitable for guided bone tissue regeneration applications in dentistry.

## 4. DISCUSSION

One of the primary roles of GBR lies in its ability to augment bone volume, particularly in areas where bone resorption has occurred due to factors such as tooth loss, trauma, or periodontal disease (Ramamurthy & Bajpai, 2024) (Priya Veeraraghavan, Rilah, et al., 2023). By providing adequate bone support, GBR facilitates optimal implant stability and osseointegration, which are vital for the long-term success of implant treatments. Moreover, GBR techniques play a crucial role in achieving favorable aesthetic outcomes. GBR also plays a pivotal role in preserving vital anatomical structures such as the maxillary sinus floor and the inferior alveolar nerve cana (Dotia et al., 2024). By preventing bone resorption and maintaining bone height and width, GBR helps mitigate the risk of complications during implant placement procedures, particularly in the posterior maxilla and mandible (Janani et al., 2021; Kachhara et al., 2021; Subramanian et al., 2023). Additionally, GBR techniques are instrumental in the treatment of peri-implantitis, a common complication characterized by inflammation and bone loss around dental implants. Through regenerative therapies, GBR aims to restore lost bone and soft tissue support, salvaging failing implants and preventing further deterioration (Gandhi et al., 2021; Katyal et al., 2023; Priyadarshini et al., 2023).

Membranes play a crucial role in excluding connective tissue cells from the bone defect site, thereby fostering selective repopulation by osteogenic cells essential for bone regeneration, such as osteoblasts and mesenchymal stem cells (Senthil, 2024). This selective cellular repopulation not only promotes new bone formation but also mitigates the risk of fibrous tissue formation, which could compromise the success of the regeneration process (Chokkattu et al., 2023; Dharman et al., 2023; Govindaraj & Shanmugam, 2023). Additionally, membranes serve to contain and stabilize bone graft materials within the defect site, facilitating optimal integration and remodeling while preventing migration or displacement of graft particles. Beyond containment, membranes also contribute to the maintenance of space and stability during the healing process, preventing collapse or distortion of the augmented area and ensuring the preservation of the desired bone architecture (Abitha et al., 2021) (Vishva et al., 2023).

According to the PASS principle which is required for a successful GBR, stabilization of the graft and membrane is essential (Rajeshkumar & Lakshmi, 2021; N. Sivakumar et al., 2021). By providing the graft in the form of electrospun membrane,



we see to it that the graft stays together and doesn't get dislodged like in particulate grafting. Furthermore, its PCL content allows it flexibility and easy adaptability to the defect site (Jang et al., 2023).

The versatility of controlling density, thickness and filler loading of electrospun membranes allows to produce a less dense higher filler loaded graft membrane and a more dense thicker barrier membrane. Furthermore as seen in the SEM images, the triangular shaped interspaces and centers of nano HAP aggregations allow invasion and binding of osteoblasts and osteoclasts. This enhances bone regeneration(E et al., 2024).

By using biomimetic nano-HAP, we are emulating the formation of nano-HAP in the human body. This allows it to be more easily absorbed and more effective in GBR(Sairaman et al., 2022).

The results of this study underscore the enhanced performance of electrospun membranes composed of PCL, PEG, and nano-hydroxyapatite (nano-HAP) for applications in guided bone tissue regeneration. The experimental data reveal significant improvements in mechanical properties, wettability, and biocompatibility when compared to the control group (PCL only).

The tensile strength and tensile strain measurements demonstrated that the addition of PEG and nano-HAP to PCL substantially improves the mechanical robustness of the electrospun membranes. The higher tensile strength and strain observed in the experiment group are indicative of better material integrity, which is essential for maintaining scaffold stability under physiological conditions. The statistically significant p-values obtained from the t-tests confirm that these improvements are not due to random variation but are a direct result of the material modifications(N. K. Sivakumar et al., 2024).

The wettability tests showed a marked decrease in the water contact angle for the experimental group compared to the control group. The lower contact angle signifies enhanced hydrophilicity, which is crucial for promoting cell adhesion, proliferation, and differentiation. Improved wettability facilitates better nutrient diffusion and waste removal, thereby creating a more favorable environment for cellular activities necessary for bone regeneration.

The confocal microscopy analysis provided clear evidence of superior cell attachment and proliferation on the PCL + PEG + nano-HAP scaffolds. The MG-63 cells displayed rapid spreading and network formation within the first few days of culture, leading to dense, multi-layered cell structures by day 7. In contrast, the control scaffolds showed relatively slower cell attachment and less dense cell layers. This suggests that the incorporation of PEG and nano-HAP significantly enhances the biocompatibility of the scaffolds, making them more effective in supporting bone tissue regeneration.

The combined effects of improved mechanical properties, enhanced wettability, and superior biocompatibility make the PCL + PEG + nano-HAP electrospun membranes highly suitable for guided bone tissue regeneration(Shah et al., 2023). These scaffolds provide a supportive matrix that mimics the extracellular matrix, promoting cellular activities essential for bone healing and regeneration. The study's findings align with the principles of guided bone regeneration (GBR), which emphasize the importance of scaffold stability, biocompatibility, and the creation of a conducive environment for bone tissue formation(Priya Veeraraghavan, Bharathidasan, et al., 2023).

While the results are promising, further research is needed to explore the long-term performance of these scaffolds in vivo. Clinical studies should be conducted to validate the efficacy of the PCL + PEG + nano-HAP membranes in actual dental implantology procedures. Additionally, optimizing the ratios of PCL, PEG, and nano-HAP could further enhance the scaffold properties and tailor them for specific clinical applications.

In general, guided bone tissue regeneration (GBTR) techniques play a vital role in facilitating bone regeneration and supporting implant stability in dental implantology. Electrospun membranes have shown great potential in these applications due to their high surface area, porosity, and tunable physical and biological properties. PCL, a biodegradable polymer with excellent biocompatibility, is commonly used in dental tissue engineering for its slow degradation rate, which aligns with the bone healing process. The addition of nano-HAP enhances the osteoconductivity of the membranes, mimicking the mineral composition of natural bone and promoting effective bone regeneration. PEG, a hydrophilic polymer, improves the processability and biocompatibility of the electrospun membranes, facilitating cell adhesion and nutrient diffusion.

The findings of this study contribute to the growing body of knowledge on the use of electrospun membranes for guided bone tissue regeneration in dentistry. The systematic methodology and comprehensive characterization provide valuable insights into the potential of these membranes to support bone regeneration and enhance the success of dental implant procedures. This research highlights the importance of material composition and structural properties in developing effective scaffolds for bone tissue engineering.

## 5. CONCLUSION

In conclusion, the preparation and characterization of electrospun membranes composed of PCL, nano-HAP, and PEG hold significant promise for guided bone tissue regeneration in dentistry. The careful selection of materials, including the biodegradable PCL, osteoconductive nano-HAP, and process-improving PEG, contributes to the creation of a membrane that aligns with the principles of GBR. The electrospinning technique enables the fabrication of nanofibrous membranes with a

structure resembling the extracellular matrix, providing a scaffold for cellular ingrowth and differentiation crucial for bone tissue formation.

## REFERENCES

- [1] Abitha, S. T., Jeevitha, M., Jayaraman, S., & Kumar, M. N. (2021). Prevalence of the use of particulate graft versus block bone graft in ridge augmentation: A hospital based retrospective study. *Journal of Pharmaceutical Research International*, 254–262.
- [2] Berton, F., Porrelli, D., Di Lenarda, R., & Turco, G. (2019). A Critical Review on the Production of Electrospun Nanofibres for Guided Bone Regeneration in Oral Surgery. *Nanomaterials (Basel, Switzerland)*, 10(1). <https://doi.org/10.3390/nano10010016>
- [3] Calciolari, E., Corbella, S., Gkraniyas, N., Viganó, M., Sculean, A., & Donos, N. (2023). Efficacy of biomaterials for lateral bone augmentation performed with guided bone regeneration. A network meta-analysis. *Periodontology 2000*. <https://doi.org/10.1111/prd.12531>
- [4] Chokkattu, J. J., Neeharika, S., Brahmajosyula, I. P., & Thangavelu, L. (2023). Comparative Evaluation Cellular Toxicity Three Heat Polymerized Acrylic Resins: Vitro Study. *World*, 14(6).
- [5] Cicciù, M., Pratella, U., Fiorillo, L., Bernardello, F., Perillo, F., Rapani, A., Stacchi, C., & Lombardi, T. (2023). Influence of buccal and palatal bone thickness on post-surgical marginal bone changes around implants placed in posterior maxilla: a multi-centre prospective study. *BMC Oral Health*, 23(1), 309.
- [6] Das, C., & Gebru, K. A. (2018). *Polymeric Membrane Synthesis, Modification, and Applications: Electro-Spun and Phase Inverted Membranes*. CRC Press.
- [7] Dharman, S., Maragathavalli, G., Shanmugam, R., & Shanmugasundaram, K. (2023). Biosynthesis Turmeric Silver Nanoparticles: Its Characterization Evaluation Antioxidant, Anti inflammatory, Antimicrobial Potential Against Oral Pathogens vitro Study. *Journal Indian Academy Oral Medicine Radiology*, 35(3), 299–305.
- [8] Doshi, K., Nivedhitha, M. S., Solete, P., Dp, S., Jacob, B., & Siddique, R. (2023). *Effect adhesive strategy universal adhesives noncarious cervical lesions-an updated systematic review meta-analysis*. *BDJ open*. 9.
- [9] Dotia, A., Selvaganesh, S., R P, A., & Nesappan, T. (2024). Dynamic Navigation Protocol for Direct Sinus Lift and Simultaneous Implant Placement: A Case Report. *Cureus*, 16(2), e53621.
- [10] Duraisamy, R., & Senior Lecturer, Department of Prosthodontics and Implantology, Saveetha Dental College and Hospitals, Saveetha Institute of Medical and Technical Sciences. (2021). Biocompatibility and Osseointegration of Nanohydroxyapatite. *International Journal of Dentistry and Oral Science*, 4136–4139.
- [11] E, D. S., Paulraj, J., Maiti, S., & Shanmugam, R. (2024). Comparative Analysis of Color Stability and Its Impact on Artificial Aging: An In Vitro Study of Bioactive Chitosan, Titanium, Zirconia, and Hydroxyapatite Nanoparticle-Reinforced Glass Ionomer Cement Compared With Conventional Glass Ionomer Cement. *Cureus*, 16(2), e54517.
- [12] Gandhi, J. M., Gurunathan, D., Doraikannan, S., & Balasubramaniam, A. (2021). Oral health status for primary dentition - A pilot study. *Journal of the Indian Society of Pedodontics and Preventive Dentistry*, 39(4), 369–372.
- [13] Givens, S. R. (2008). *The Effect of Solvent Properties on Electrospun Polymer Fibers and Applications in Biomaterials*.
- [14] Govindaraj, P., & Shanmugam, R. (2023). Effect chlorhexidine fluoride varnish incidence white spot lesion orthodontic patients. *Annals Dental Specialty*, 11(1-2023), 35–39.
- [15] Hilal, N., Ismail, A. F., Matsuura, T., & Oatley-Radcliffe, D. (2017). *Membrane Characterization*. Elsevier.
- [16] Janani, K., Teja, K. V., & Ajitha, P. (2021). Cytotoxicity of oregano essential oil and calcium hydroxide on L929 fibroblast cell: A molecular level study. *Journal of Conservative Dentistry: JCD*, 24(5), 457–463.
- [17] Jang, H. J., Kang, M. S., Kim, W.-H., Jo, H. J., Lee, S.-H., Hahm, E. J., Oh, J. H., Hong, S. W., Kim, B., & Han, D.-W. (2023). 3D printed membranes of polylactic acid and graphene oxide for guided bone regeneration. *Nanoscale Advances*, 5(14), 3619–3628.
- [18] Jawaaid, M., Thariq, M., & Saba, N. (2018). *Mechanical and Physical Testing of Biocomposites, Fibre-Reinforced Composites and Hybrid Composites*. Woodhead Publishing.
- [19] Kachhara, S., Nallaswamy, D., Ganapathy, D., & Ariga, P. (2021). Comparison of the CBCT, CT, 3D printing, and CAD-CAM milling options for the most accurate root form duplication required for the root analogue implant (RAI) protocol. *Journal of Indian Academy of Oral Medicine and Radiology*, 33(2), 141–145.
- [20] Kandhari, S., Khalid, S., James, A., & Laverty, D. P. (2023). Bone grafting techniques and materials for implant

dentistry. *British Dental Journal*, 235(3), 180–189.

- [21] Katyal, D., Jain, R. K., Sankar, G. P., & Prasad, S. (2023). Antibacterial, Cytotoxic, Mechanical Characteristics Novel Chitosan-Modified Orthodontic Primer: : In-Vitro: Study. *Journal International Oral Health*, 15(3), 284–289.
- [22] Lampl, S., Gurunathan, D., Krithikadatta, J., Mehta, D., & Moodley, D. (2023). Reasons for Failure of CAD/CAM Restorations in Clinical Studies: A Systematic Review and Meta-analysis. *The Journal of Contemporary Dental Practice*, 24(2), 129–136.
- [23] Lee, J.-H., An, H.-W., Im, J.-S., Kim, W.-J., Lee, D.-W., & Yun, J.-H. (2023). Evaluation of the clinical and radiographic effectiveness of treating peri-implant bone defects with a new biphasic calcium phosphate bone graft: a prospective, multicenter randomized controlled trial. *Journal of Periodontal & Implant Science*, 53(4), 306–317.
- [24] Liang, C., Wang, G., Liang, C., Li, M., Sun, Y., Tian, W., & Liao, L. (2024). Hierarchically patterned triple-layered gelatin-based electrospun membrane functionalized by cell-specific extracellular matrix for periodontal regeneration. *Dental Materials: Official Publication of the Academy of Dental Materials*, 40(1), 90–101.
- [25] Mahmoud, A. H., Han, Y., Dal-Fabbro, R., Daghrery, A., Xu, J., Kaigler, D., Bhaduri, S. B., Malda, J., & Bottino, M. C. (2023). Nanoscale  $\beta$ -TCP-Laden GelMA/PCL Composite Membrane for Guided Bone Regeneration. *ACS Applied Materials & Interfaces*, 15(27), 32121–32135.
- [26] Pandiyan, I., Arumugham, M. I., Doraikannan, S. S., Rathinavelu, P. K., Prabakar, J., & Rajeshkumar, S. (2023). Antimicrobial and Cytotoxic Activity of Ocimum tenuiflorum and Stevia rebaudiana-Mediated Silver Nanoparticles - An In vitro Study. *Contemporary Clinical Dentistry*, 14(2), 109–114.
- [27] Pavithra, S., Paulraj, J., Rajeshkumar, S., & Maiti, S. (2023). Comparative evaluation antimicrobial activity compressive strength conventional thyme-modified glass ionomer cement. *Annals Dental Specialty*, 11(1-2023), 70–77.
- [28] Priyadarshini, G., Gheena, S., Ramani, P., Rajeshkumar, S., & Ramalingam, K. (2023). Assessment antimicrobial efficacy cytotoxicity Cocos nucifera Triticum aestivum combination gel formulation therapeutic use. *World Journal Dentistry*, 14(5), 414–418.
- [29] Priya Veeraghavan, V., Bharathidasan, P., Gayathri, R., & Kavitha. (2023). Biogenic Selenium nanoparticles loaded alginate-gelatin scaffolds for potential tissue engineering applications. *Texila International Journal of Public Health*, 86–93.
- [30] Priya Veeraghavan, V., Rilah, K., Gayathri, R., & Kavitha. (2023). Fabrication, characterization, antibacterial and biocompatibility studies of graphene oxide loaded alginate chitosan scaffolds for potential biomedical applications. *Texila International Journal of Public Health*, 77–85.
- [31] Rajeshkumar, S., & Lakshmi, T. (2021). Green synthesis gold nanoparticles using kalanchoe pinnata its free radical scavenging activity. *Int J Dentistry Oral Sci*, 8(7), 2981–2984.
- [32] Ramamurthy, J., & Bajpai, D. (2024). Role of alginate-based scaffolds for periodontal regeneration of intrabony defects: A systematic review. *World Journal of Dentistry*, 15(2), 181–187.
- [33] Ramsundar, K., Jain, R. K., Balakrishnan, N., & Vikramsimha, B. (2023). Comparative evaluation bracket bond failure rates novel non-primer adhesive conventional primer-based orthodontic adhesive-a pilot study. *Journal Dental Research*, 17(1).
- [34] Rieshy, V., Chokkattu, J. J., Rajeshkumar, S., & Neeharika, S. (2023). Mechanism action clove ginger herbal formulation-mediated TiO<sub>2</sub> nanoparticles against lactobacillus species: vitro study. *Journal Advanced Oral Research*, 14(1), 61–66.
- [35] Sairaman, S., Nivedhitha, M. S., Shrivastava, D., Al Onazi, M. A., Algarni, H. A., Mustafa, M., Alqahtani, A. R., AlQahtani, N., Teja, K. V., Janani, K., Eswaramoorthy, R., Sudhakar, M. P., Alam, M. K., & Srivastava, K. C. (2022). Biocompatibility and antioxidant activity of a novel carrageenan based injectable hydrogel scaffold incorporated with Cissus quadrangularis: an in vitro study. *BMC Oral Health*, 22(1), 377.
- [36] Senthil, R. (2024). Silk fibroin sponge impregnated with fish bone collagen: A promising wound healing scaffold and skin tissue regeneration. *The International Journal of Artificial Organs*, 47(5), 338–346.
- [37] Shah, T., Surendar, S., & Singh, S. (2023). Green Synthesis of Zinc Oxide Nanoparticles Using Ananas comosus Extract: Preparation, Characterization, and Antimicrobial Efficacy. *Cureus*, 15(10), e47535.
- [38] Shankar, P., Arumugam, P., & Kannan, S. (2024). Development, characterisation and biocompatibility analysis of a collagen-gelatin-hydroxyapatite scaffold for guided Bone Regeneration. *Odovtos - International Journal of Dental Sciences*, 235–248.



- [39] Shenoy, A., Maiti, S., Nallaswamy, D., & Keskar, V. (2023). An in vitro comparison of the marginal fit of provisional crowns using the virtual tooth preparation workflow against the traditional technique. *Journal of Indian Prosthodontic Society*, 23(4), 391–397.
  - [40] Singh, S., Prasad, A. S., & Rajeshkumar, S. (2023). Cytotoxicity, antimicrobial, anti-inflammatory and antioxidant activity of camellia sinensis and citrus mediated copper oxide nanoparticle-an in vitro study. *Journal of International Society of Preventive & Community Dentistry*, 13(6), 450–457.
  - [41] Sivakumar, N., Geetha, R. V., Priya, V., Gayathri, R., & Ganapathy, D. (2021). Targeted phytotherapy for reactive oxygen species linked oral cancer. *Int J Dent Oral Sci*, 8.
  - [42] Sivakumar, N. K., Palaniyappan, S., Vishal, K., Alibrahim, K. A., Alodhayb, A., & Kumar, M. (2024). Crushing behavior optimization of octagonal lattice-structured thin-walled 3D printed carbon fiber reinforced PETG (CF/PETG) composite tubes under axial loading. *Polymer Composites*, 45(2), 1228–1249.
  - [43] Subramanian, A. K., Lalit, H., & Sivashanmugam, P. (2023). Preparation, characterization, and evaluation of cytotoxic activity of a novel titanium dioxide nanoparticle-infiltrated orthodontic adhesive: An in vitro study. *World Journal of Dentistry*, 14(10), 882–887.
  - [44] Su, H. (2020). *IN VITRO AND IN VIVO EVALUATION AND MECHANICAL IMPROVEMENT OF THE ELECTROSPUN CHITOSAN MEMBRANE*.
  - [45] Thomas, & Jain, R. K. (2023). Influence operator experience scanning time accuracy two different intraoral scanners-a prospective clinical trial. *Turkish Journal Orthodontics*, 36(1).
  - [46] Tolstunov, L. (2022). *Essential Techniques of Alveolar Bone Augmentation in Implant Dentistry: A Surgical Manual*. John Wiley & Sons.
  - [47] Tripathi, G., Ho, V. H., Jung, H.-I., & Lee, B.-T. (2023). Physico-mechanical and in-vivo evaluations of tri-layered alginate-gelatin/polycaprolactone-gelatin- $\beta$ -TCP membranes for guided bone regeneration. *Journal of Biomaterials Science. Polymer Edition*, 34(1), 18–34.
  - [48] Vishva, P., R, N., & Harikrishnan, S. (2023). The Effect of Platelet-Rich Plasma on Bone Volume in Secondary Alveolar Bone Grafting in Alveolar Cleft Patients: A Systematic Review. *Cureus*, 15(9), e46245.
  - [49] Watcharajittanont, N., Putson, C., Pripatnanont, P., & Meesane, J. (2023). Corrigendum: Layer-by-layer electrospun membranes of polyurethane/silk fibroin based on mimicking of oral soft tissue for guided bone regeneration (201914 055011). *Biomedical Materials*, 18(5). <https://doi.org/10.1088/1748-605X/ace6e7>
  - [50] Wu, V., Klein-Nulend, J., Bravenboer, N., Ten Bruggenkate, C. M., Helder, M. N., & Schulten, E. A. J. M. (2023). Long-Term Safety of Bone Regeneration Using Autologous Stromal Vascular Fraction and Calcium Phosphate Ceramics: A 10-Year Prospective Cohort Study. *Stem Cells Translational Medicine*, 12(9), 617–630.
-